

Recurrence quantification analysis of turbulent fluctuations in the plasma edge of Tokamak Chauffage Alfvén Brésilien tokamak

Z. O. Guimarães-Filho,^{1,a)} I. L. Caldas,¹ R. L. Viana,^{2,b)} I. C. Nascimento,¹ Yu. K. Kuznetsov,¹ and J. Kurths³

¹Instituto de Física, Universidade de São Paulo, 05315-970 São Paulo, São Paulo, Brazil

²Departamento de Física, Universidade Federal do Paraná, 81531-990 Curitiba, Paraná, Brazil

³Humboldt Universität, Berlin 10115, Germany

(Received 7 August 2009; accepted 8 December 2009; published online 14 January 2010)

Recurrences are close returns of a given state in a time series, and can be used to identify different dynamical regimes and other related phenomena, being particularly suited for analyzing experimental data. In this work, we use recurrence quantification analysis to investigate dynamical patterns in scalar data series obtained from measurements of floating potential and ion saturation current at the plasma edge of the Tokamak Chauffage Alfvén Brésilien [R. M. O. Galvão *et al.*, Plasma Phys. Controlled Fusion **43**, 1181 (2001)]. We consider plasma discharges with and without the application of radial electric bias, and also with two different regimes of current ramp. Our results indicate that biasing improves confinement through destroying highly recurrent regions within the plasma column that enhance particle and heat transport. © 2010 American Institute of Physics. [doi:10.1063/1.3280010]

I. INTRODUCTION

Electrostatic turbulence in the tokamak plasma edge is a likely candidate for explaining cross-field anomalous transport¹ and it is also important to describe plasma-wall interactions in tokamaks.² Anomalous transport is dominated by instabilities driven by strong temperature and density gradients along radial directions (i.e., directions normal to the magnetic flux surfaces).³ These instabilities can be experimentally investigated through measurements of fluctuations of quantities such as electrostatic potential and ion saturation currents using probes. From these measurements we can obtain the fluctuating radial plasma velocity through $\mathbf{E} \times \mathbf{B}$ drift and radial particle fluxes.⁴ The broadband electrostatic fluctuations observed in the tokamak plasma edge present some distinctive features of fully-developed turbulence with fluctuation levels in the 10%–30% range.³ Quantifying electrostatic turbulence is thus essential to get physically interesting information on the quantities derived from these measurements.

However, this problem is far from being simple. Typical time series obtained from floating potential or ion saturation current measurements are not just purely stochastic signals but rather intermittent series punctuated by large and sporadic events. Hence a conventional statistical approach, based only on the properties of the probability distribution function of the fluctuating data, may be not enough to quantify the strength of the turbulent electrostatic fluctuations.

On the other hand, these series exhibit a behavior akin of complex systems, where features of both ordered and disordered dynamics are simultaneously present, with an interplay

of energy among temporal and spatial degrees of freedom.⁵ We usually call this phenomenon as structure formation in turbulent signals, which carry on valuable information on the deterministic factors which, in addition to stochastic ones, compose complex time series.^{6,7} The structures, on their hand, can be related to physical processes described by classical or neoclassical theories, such as drift-wave turbulence.¹ One of the advantages of having some knowledge about these structures is to open the possibility of an effective control procedure aiming to decrease the turbulence levels in order to improve transport properties at the tokamak edge.^{3,8}

In this paper we pursue a different approach, the recurrence quantification analysis (RQA), widely used in nonlinear dynamics,⁹ in order to quantify complex signals such as those yielded by electrostatic turbulence, and which is based on the recurrence properties of the time series.¹⁰ The key idea in RQA is recurrence, which is a basic property of dynamical systems as already introduced by Poincaré in 1890: in volume-preserving flows with bounded orbits only, a given state will return, after a sufficiently long time, to an arbitrarily small neighborhood of this state. Even though our system does not fulfill the requirements for the Poincaré recurrence theorem, we can exploit the idea of recurrence by tracking the evolution of the systems state at each time, in order to find the instant where it returns close to that state.⁵

The matching of possible recurrences among all time instants for a given time series leads to a recurrence matrix, whose graphical representation is called a recurrence plot (RP), and has been introduced in nonlinear dynamics to calculate the maximum Lyapunov exponent related to a time series,¹¹ as well as to study its nonstationarity.¹² The structures that have been identified in RPs allow the use of RQA,¹³ which has been extensively used in many applications in meteorology,¹⁴ finance,¹⁵ geophysics,¹⁶ and

^{a)}Present address: PIIM, Université de Provence, F-13397 Marseille Cedex 20, France.

^{b)}Author to whom correspondence should be addressed. Electronic mail: viana@fisica.ufpr.br.

cardiology.¹⁷ There are also some applications of RPs in space^{18,19} and fusion plasmas as well.¹⁰

In this work we use RQA to characterize and quantify the recurrence content of electrostatic fluctuations in the edge region of a tokamak, using data obtained from measurements made in the Tokamak Chauffage Alfvén Brésilien (TCABR).²⁰ By tokamak edge we mean the region near to the last closed flux surface, including the scrape-off layer. Probes have been built in TCABR to measure the electrostatic potential and ion saturation current fluctuations in the edge region, giving information on plasma potential and particle density.²¹

Electrostatic fluctuations in the plasma edge have been assigned to physical processes governed by nonlinear mechanisms, such as the interaction between drift waves, which appear due to the steep density gradients in the tokamak edge region.^{1,22,23} These interactions exhibit a strong dependence on the radial variable, which is reflected in the turbulent fluctuation levels measured in the experiments. One of the main aims of the present paper is to use RQA to quantify the radial variation of the recurrences present in turbulent fluctuations.

There are yet other factors affecting plasma edge turbulence which have been tested in TCABR. One of them is the use of a voltage biased electrode inserted at the tokamak edge in order to improve plasma confinement.²⁴ In a previous paper¹⁰ we considered the radial variation of turbulent fluctuations for tokamak discharges without electrode biasing, finding that the presence of structures in the recurrences of the floating potential fluctuations is higher just after the plasma radius. In this paper we substantially extend the previous analysis and use the RQA to detect variations on the radial profile of turbulence recurrence due to biasing, considering also qualitatively different regimes, which differ by the different plasma current evolution during the early phase of the discharges.²⁵

The paper is organized as follows: in the Sec. II we outline the basic concepts of RPs and RQA, respectively. Section III deals with the experimental setup and the kind of data we obtain from the tokamak TCABR. The application of RQA to turbulent series of floating potential in discharges before and during biasing is treated in Sec. IV with special emphasis on quantifying the signals recurrence. Section V shows the recurrence radial dependence for other turbulent signals during these two conditions, and also compares two different regimes of operation in TCABR, which differ by the evolution of plasma current. Section VI contains our conclusions and suggestions for further work.

II. RECURRENCE QUANTIFICATION ANALYSIS

We consider the time series obtained by measuring the electrostatic fluctuations in the tokamak plasma edge $y_i = y(t=i\Delta)$ at a given space point, where Δ is the inverse sampling frequency, and $i=1, 2, \dots, N$ (N is the total number of points). We make an embedding using time-delay coordinates from which we form the vectors $\mathbf{y}_i = \{y_i, y_{i+\tau}, y_{i+2\tau}, \dots, y_{i+(d-1)\tau}\}$ belonging to a d -dimensional reconstructed phase space, where d is the embedding dimen-

sion and τ is the delay.²⁶ The embedding dimension and the time delay can be estimated, respectively, from the method of false neighbors and the first zero of the autocorrelation function.²⁷

A recurrence occurs whenever a trajectory visits roughly the same d -dimensional volume in the reconstructed phase space. A RP depicts, at a given instant, the times at which $\mathbf{y}_i \approx \mathbf{y}_j$, where $i=1, 2, \dots, N$ is represented in the horizontal axis, and j with the same range in the vertical axis. More formally, we construct a recurrence matrix by comparing embedding vectors with each other at different times, drawing pixels when the distance between vectors falls within an ϵ -neighborhood^{11,28-31} $\mathbf{R}_{i,j} = H(\epsilon - \|\mathbf{y}_i - \mathbf{y}_j\|)$, ($i, j=1, 2, \dots, N$), where ϵ is a threshold, $H(\cdot)$ is the Heaviside unit step function, and $\|\cdot\|$ stands for some norm, e.g., the Euclidean norm. The RP is thus obtained by assigning a black (white) dot to the points for which $\mathbf{R}_{i,j}=1(0)$. By construction, the recurrence matrix is symmetric ($\mathbf{R}_{i,j}=\mathbf{R}_{j,i}$), and a point is always recurrent to itself, i.e., $\mathbf{R}_{i,i}=1$, forming the main diagonal line.

RQA is a set of quantitative procedures to identify and characterize dynamical behavior using RPs, based in three basic kinds of structures: (i) isolated points; (ii) diagonal lines; and (iii) horizontal and vertical lines.⁹ In order to quantify these structures, RQA offers a variety of numerical diagnostics.³² The recurrence rate (RR) is the probability of finding a black recurrence point (for which $\mathbf{R}_{i,j}=1$) or

$$\text{RR} = \frac{1}{N(N-1)} \sum_{i,j=1; i \neq j}^N \mathbf{R}_{i,j}, \quad (1)$$

where N^2 is the total number of pixels in a RP.³³ Diagonal lines of length ℓ are parallel to the main diagonal line. In RPs they appear with various lengths, so that we compute $P(\ell) = \{\ell_i; i=1, 2, \dots, N_\ell\}$, which is the frequency distribution of the lengths ℓ_i of diagonal lines, N_ℓ being its absolute number with the exception of the main diagonal line.³⁴ Since the presence of diagonal lines is usually related with deterministic behavior, the fraction of points in a RP belonging to diagonal lines is called determinism (DET), defined as

$$\text{DET} = \frac{\sum_{\ell=\ell_{\min}}^{\ell_{\max}} \ell P(\ell)}{\sum_{i,j=1; i \neq j}^N \mathbf{R}_{i,j}}, \quad (2)$$

where ℓ_{\min} is the minimum length allowed for a diagonal line, whereas the *maximum diagonal length* is $\ell_{\max} = \max\{\ell_i, i=1, 2, \dots, N_\ell\}$. A related quantity is the *average diagonal length* (Ldm)

$$\text{Ldm} = \frac{\sum_{\ell=\ell_{\min}}^{\ell_{\max}} \ell P(\ell)}{\sum_{\ell=\ell_{\min}}^{\ell_{\max}} P(\ell)}. \quad (3)$$

We can use RPs to compute reliable estimates for the *Shannon entropy* (ENTR) of the distribution of the diagonal lengths

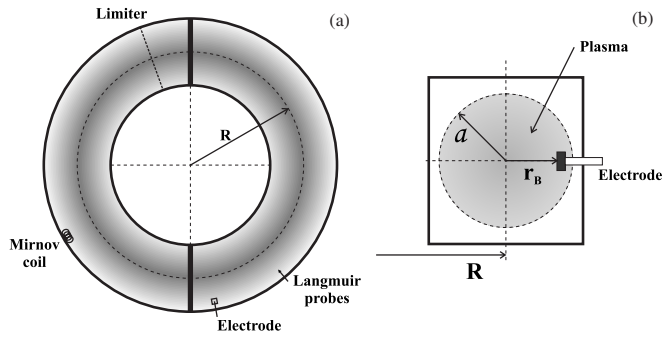


FIG. 1. Scheme of the experimental setup: (a) viewed from above and (b) cross-sectional view.

$$\text{ENTR} = - \sum_{\ell=\ell_{\min}}^{\ell_{\max}} p(\ell) \ln p(\ell), \quad (4)$$

where

$$p(\ell) = \frac{P(\ell)}{\sum_{\ell=\ell_{\min}}^{\ell_{\max}} P(\ell)}, \quad (5)$$

is the probability distribution of the diagonal line lengths. ENTR reflects the complexity of the deterministic structure in the system.

The length of a vertical line measures the duration of a laminar state (or a state which does not change much with time). Vertical lines of length v have a probability distribution function $P(v) = \{v_i; i=1, 2, \dots, N_v\}$, where N_v is the absolute number of vertical lines. The *laminarity* (LAM) is the percentage of RP points forming vertical lines

$$\text{LAM} = \frac{\sum_{v=v_{\min}}^{v_{\max}} vP(v)}{\sum_{i,j=1; i \neq j}^N \mathbf{R}_{i,j}}, \quad (6)$$

where v_{\min} is the minimum lengths of a vertical line, whereas the maximum vertical length is $v_{\max} = \max(\{v_i, i=1, 2, \dots, N_v\})$. The *trapping time* (TT) is the average length of a vertical line

$$\text{TT} = \frac{\sum_{v=v_{\min}}^{v_{\max}} vP(v)}{\sum_{v=v_{\min}}^{v_{\max}} P(v)}. \quad (7)$$

III. EXPERIMENTAL SETUP

The experimental results to be studied in this work were obtained from a hydrogen circular plasma produced in the ohmically heated Brazilian tokamak TCABR (Ref. 20) (major radius $R=61$ cm and minor radius $a=18$ cm). The plasma current reaches a maximum value of 100 kA, with a duration 100 ms, the hydrogen filling pressure is 3×10^{-4} Pa, and the toroidal magnetic field $B_T=1.1$ T. At the scrape-off layer, the electron plasma density is $n_e \approx 1.5 \times 10^{18}$ m $^{-3}$, and the electron temperature is $T_e \approx 5$ eV.

Three Langmuir probes measure electrostatic fluctuations within the tokamak plasma outer region. Two of these probes measure the floating potential fluctuations and the

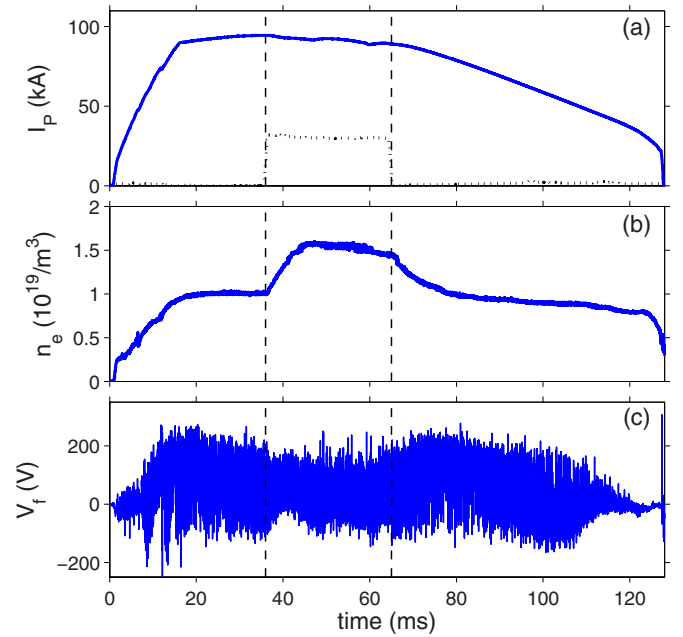


FIG. 2. (Color online) Time evolution of (a) plasma current, (b) electron density, and (c) floating potential for a typical discharge of TCABR tokamak. The vertical lines indicate the interval during which biasing is applied to the plasma. The dotted line in (a) indicates the applied bias current.

third probe measures the ion saturation current fluctuations.²¹ The whole set was mounted at the outer equatorial region of the tokamak [Fig. 1(a)]. The measurements were performed at the region comprising the plasma edge and the scrape-off layer ($r \approx a$). The probes are mounted on a movable shaft that can be displaced radially from $r=16.5$ cm to 21.0 cm with respect to the center of the plasma column. The probe displacement, however, occurs only for separate discharges, in order not to disturb the plasma due to the movement of the probe. Probe data were digitized at 1 megasample/s and filtered by a 300 kHz antialiasing filter. The electrode was positioned 1.5 cm inside the plasma ($r/a=0.92$), at the equatorial plane and low field side of the plasma column, 160° from the graphite limiter in the plasma current direction (counterclockwise top view) [Fig. 1(b)].

Figure 2 shows the time evolution of a typical tokamak plasma discharge in TCABR. The plasma current [Fig. 2(a)] grows rapidly in the first 20 ms and reaches a plateau where the current stays at a 100 kA level, decaying slowly during the second half until the eventual disrupture. The central estimated electron density, indicated by Fig. 2(b), exhibits a similar increase during the first 20 ms with a first plateau level of $n_e \sim 1.0 \times 10^{19}$ m $^{-3}$. The dc-bias is switched on at 37 ms and is kept active during the next 29 ms, a time interval indicated by vertical bars in the discharge depicted in Fig. 2(a).

Just after the dc-bias has been started, the electron density experiences a fast increase and achieves a second plateau of $\sim 1.5 \times 10^{19}$ m $^{-3}$, which persists during the application of the dc-bias and even for a short time after it has been switched off. This regime of high electron density has some features in common with H-mode confinement. With the Langmuir probes described above there were measured the

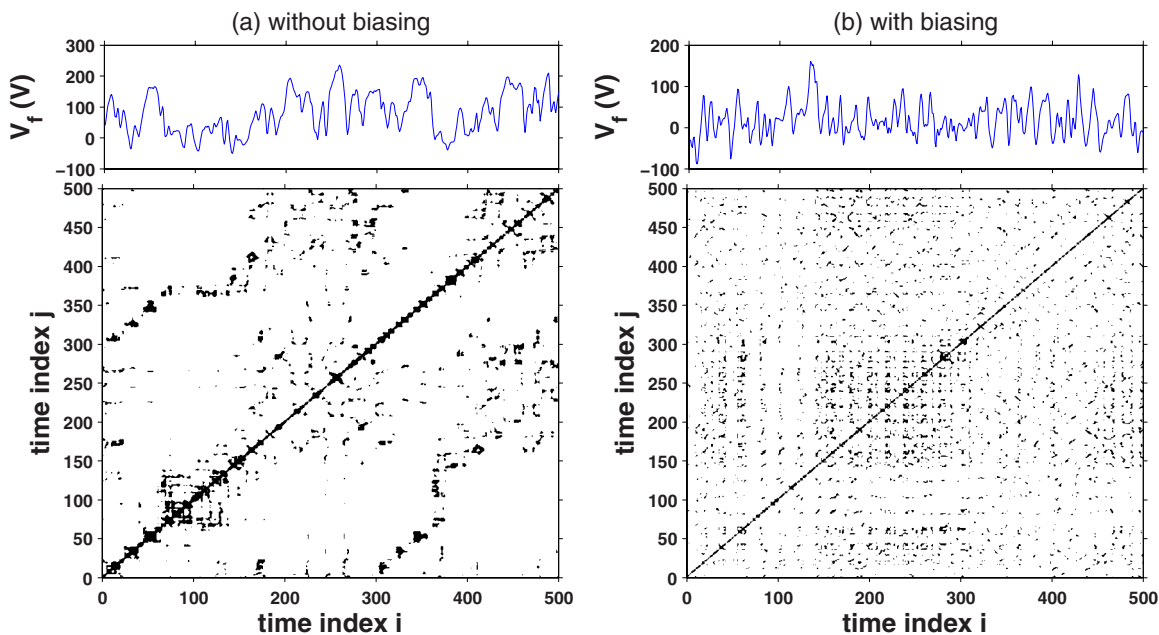


FIG. 3. (Color online) Time series and corresponding RPs for floating potential data measured (a) without and (b) with biasing.

floating potential V_f in the plasma edge, a typical profile being depicted in Fig. 2(c). The featured signal exhibits highly irregular fluctuations from -200 to $+200$ V range.

A visual inspection of Fig. 2(c) suggests that the amplitude of the floating potential oscillations undergo a slight decrease just after biasing. On the other hand, a linear data analysis using conventional techniques, e.g., spectral analysis, is also able to evidence some changes in the floating potential fluctuations with and without biasing. For example, after biasing the low-frequency components of the fluctuation spectra become weaker. Hence, we claim that recurrence-based diagnostics are complementary to conventional methods, but having some advantages over spectral analysis.

One of these advantages is that spectral analysis is particularly suitable for linear processes, whereas turbulent fluctuations are known to originate from highly nonlinear processes occurring in the plasma itself as well as the magnetic field used to confine it. Hence a signature of bias in the electrostatic turbulence data should be looked for using procedures suitable to analyze data from nonlinear processes. This happens to be the case of recurrence plots, which harness the recurrent property of chaotic orbits in the phase space. This will be used in Sec. IV to evidence traces of biasing in the turbulent data, which would be elusive otherwise with linear methods of characterization.

IV. ELECTROSTATIC TURBULENCE IN DISCHARGES WITH AND WITHOUT BIASING

Electrostatic turbulent data are expected to be generated by nonlinear systems undergoing complex behavior in space and time, particularly chaotic behavior over an extended realm in space.^{1,23,35,36} This means that it is usually difficult to predict the effect of a given perturbation on the output of turbulent measurements. The absence of linearity may cause

that a given increase in an external source of energy does not produce an effect of the same magnitude, or even it may not cause an effect at all (as in the case of nonlinear saturation). There are two basic types of changes in turbulent data: qualitative and quantitative ones, the latter being related to the (spatiotemporal) dynamics of the physical processes generating the data.

The detection of quantitative changes using linear approaches such as power spectra is naturally limited in view of the strong nonlinear character of plasma turbulence, and encourages the use of diagnostics more appropriate to complex systems, such as the correlation dimension, Lyapunov exponents, or entropies.²⁷ However, the existing methods for evaluating those quantities assume that the time series being investigated is stationary, very long, and with only low noise. These requirements are usually impossible to fulfill in plasma experiments. The TCABR analyzed data, for example, are quasistationary since the plasma parameters (as the plasma current and electron density, shown in Fig. 2) vary slowly with respect to the typical dominant fluctuation periods. This condition is fulfilled by choosing windows of 0.5 ms duration, each of them corresponding to 500 sampled data points.

In the specific case of the effect of biasing on the floating potential turbulent oscillations, the recurrence plots for the considered window of two time series, with and without biasing, are depicted in Fig. 3. The corresponding time series is plotted above the RP for the sake of visualization. As mentioned in Sec. III, with respect to Fig. 2(c), a qualitative change that is quite easy to detect is that, during biasing, the overall amplitude of fluctuations decreases, when compared to the same fluctuations without biasing. However, by the present reasoning, this diagnostic does not lead to further conclusions about the intensity or even the noise levels re-

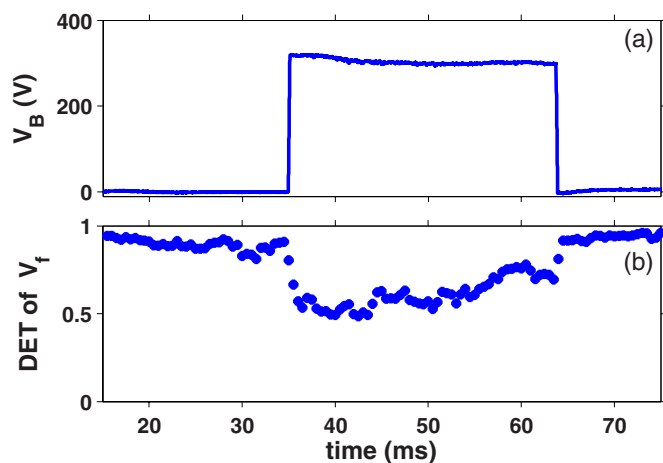


FIG. 4. (Color online) Time evolution of the (a) bias potential and (b) determinism of floating potential data in windows of 1 ms.

lated to the dynamics of the process occurring during bias in the plasma.

The recurrence plots depicted in Fig. 3 were obtained by choosing the embedding dimension as $d=4$ and the time delay $\tau=20 \mu\text{s}$ was selected by considering that the autocorrelation function is less than $1/e$ in most signals.²⁷ Instead of fixing the threshold radius ϵ (in order to consider two points as being recurrent or not), we fixed the RR so as to uniformize recurrence plots obtained from different kinds of data. In other words, we consider two points as being recurrent or not depending on the overall RR of the series be equal to some given value, like, e.g., 5.0%, which we shall use throughout this work. Hence, if most points are so close that they would be considered recurrent if a fixed threshold be given with a fixed RR they will be recurrent only if their contribution falls into that percentage.

We can recognize even visually substantial changes in the turbulent behavior at the plasma edge by comparing the diagonal and vertical structures of Fig. 3(a) (without bias) with the scattered nature of the recurrence plots depicted by Fig. 3(b) (with bias), which suggests a reduction in the deterministic effect, probably related to the existence of a lower number of large-scale structures due to the biasing. A quantitative assessment of this reduction, however, is provided by RQA.

To evaluate this reduction, in Fig. 4(b) we show the time evolution of DET, the corresponding bias voltage being plotted in Fig. 4(a) for ease of comparison. Each point in Fig. 4(b) represents the result of Eq. (2), as applied to a single RP constructed from consecutive pieces of an original series [see Fig. 3], each of them with 1 ms of length (equivalent to 1000 points). The decrease in DET (by almost a factor of two) is evident just after biasing starts being applied, and resumes its previous values just as biasing is switched off. Such a decrease in DET can be assigned to substantial destruction of structures of the RPs during biasing, a fact that cannot be recognized by a simple inspection of the corresponding original time series in Fig. 3. Moreover, this decrease should result from a deep dynamical change in the physical process producing the turbulent data.

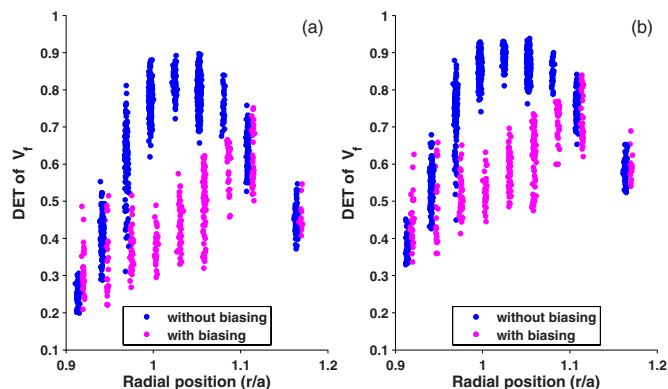


FIG. 5. (Color online) Radial profile of determinism for floating potential data before [blue (black) points] and during biasing [red (gray) points]. Each point represents a window of 1 ms. The RR was fixed on (a) 2.5% and (b) 5.0%.

V. RADIAL DEPENDENCE OF RECURRENCE PROPERTIES OF ELECTROSTATIC TURBULENCE DATA

The electrostatic turbulence properties are not uniform over the plasma edge, and we used RQA to evaluate this dependence along the radial direction. Initially we have used the determinism so as to investigate such variation, our results being shown in Fig. 5, where the DET has been computed for signals measured at different radial positions and for several discharges, according to the experimental protocol exposed in Sec. III. Each recurrence plot, for a given radial position, is represented by different points. This choice makes it possible to observe not only the average-variation but also because it gives an idea of the actual distribution of results. Blue (black) in Fig. 5 points represent measured data without biasing, and their radial profile shows an increase as we approach the plasma radius (at $r=a$) with a maximum value just after that location already within the scrape-off layer. After that, we found that DET decreases as we cross the scrape-off layer and approach the tokamak wall.¹⁰ Hence the turbulent fluctuations become weaker, as we move outside the plasma radius toward the vessel wall.

With biasing [red (gray) points], however, the radial profile of DET suffers a radical change. First DET decreases the most where it is more intense, namely at the vicinity of plasma edge, an effect possibly caused by the breakup of coherent large-scale structures in that region. In the second place, this alteration occurs over a wide radial interval. The difference between Figs. 5(a) and 5(b) is that the RR has been fixed as 2.5% and 5.0%, respectively. This is a strong indication that our results are not artifacts of a too small or too large threshold radius ϵ , and rather represent “truly” recurrent points. Similar changes in values, but not in the trend, were previously observed for discharges without biasing by varying the embedding dimension used to reconstruct the phase space of the system.¹⁰

Other quantifiers from RQA would present similar results, as shown in Fig. 6, with and without biasing. The radial profiles of laminarity (6) [Fig. 6(a)], Shannon entropy (4) [Fig. 6(b)], average diagonal length (3) [Fig. 6(c)], and trapping time (7) [Fig. 6(d)] show the characteristic increase

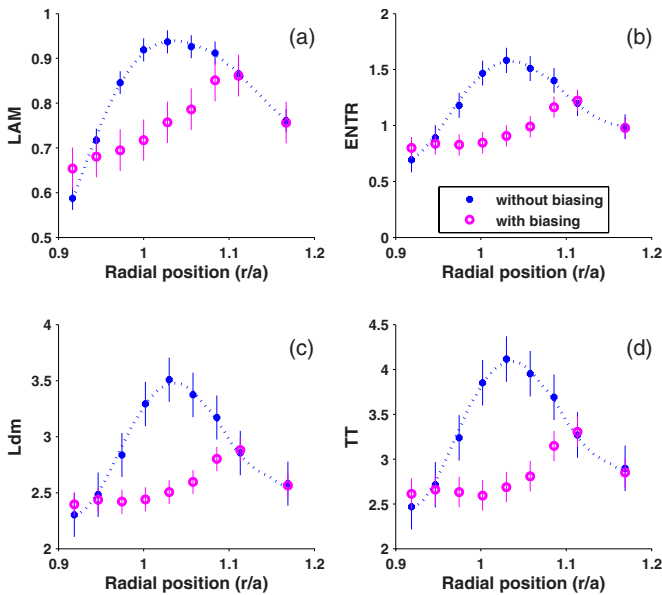


FIG. 6. (Color online) Radial profile of (a) laminarity, (b) entropy, (c) average laminar length, and (d) trapping time for floating potential data before (filled circles) and during biasing (open circles). The indicated values are the averages and the error bars represent the standard deviation with respect to these averages.

in fluctuation recurrence, as we approach the plasma radius from the plasma core, and its decrease, as we move toward the tokamak wall. Moreover, all the other quantifiers obtained from RQA reinforce the flattening of the radial profiles with biasing [red (gray) points], meaning that the largest reduction comes, as a trend from the larger values of the quantifiers, so yielding a large region of change. In spatial terms, the dynamical change is clearly not a local but rather a global feature of the plasma edge region as a whole.

These results indicate that the recurrence-based results obtained from RQA cannot be taken from themselves, but rather should complement conventional (e.g., spectral or bispectral) methods with whom they may be compared with get a better picture of the changes we observe in fluctuations due to various processes in the plasma.²³ In a recent paper³⁷ there were used multifractal diagnostics to investigate edge turbulence, finding similarities between the radial profiles obtained from recurrence-based and Hurst exponent (considering floating potential fluctuations in discharges without biasing).

Besides the floating potential, the Langmuir probes have also been used to measure the ion saturation current fluctuation at different positions in the plasma edge. In Figs. 7(a) and 7(b), we compare the radial profiles of floating potential and ion saturation current data, respectively, with and without biasing. Unlike the potential, the ion saturation current has a quasimonotonic increase as we approach the tokamak wall, with almost constant values in the scrape-off layer. The presence of biasing decreases DET, as before, and the profile seems to be flattened near the plasma radius, and continues to increase in the scrape-off layer, both for V_f and I_S data.

The electrostatic potential fluctuations lead to poloidal electric field \tilde{E}_θ oscillations and thus to a fluctuating radial drift velocity $\tilde{v}_r = \tilde{E}_\theta / B_T$.¹ This $\mathbf{E} \times \mathbf{B}$ -drift, on its hand, pro-

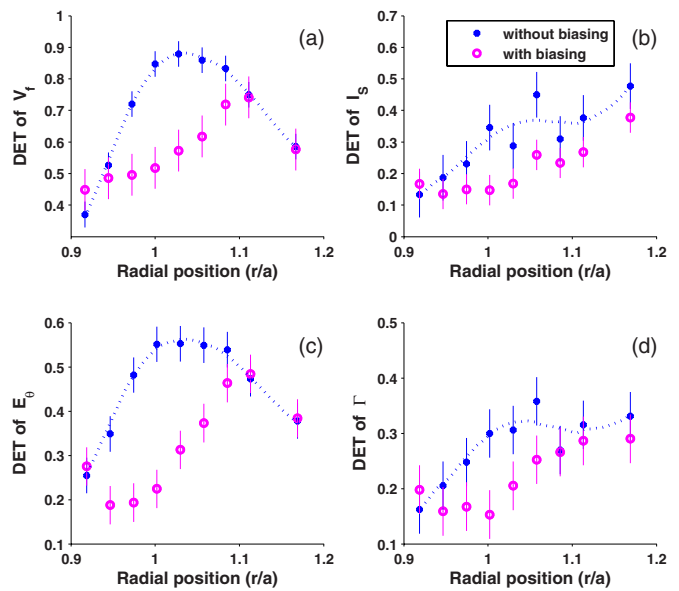


FIG. 7. (Color online) Radial profile of determinism for (a) floating potential, (b) fluctuating ion saturation current, (c) poloidal electric field, and (d) turbulence driven particle transport flux before (filled circles) and during biasing (open circles).

duces a radial particle flux $\Gamma = \langle \tilde{n} \tilde{v}_r \rangle$, where the density fluctuations are proportional to the ion saturation current fluctuations ($\tilde{n} \sim \tilde{I}_S$), on neglecting the temperature fluctuations. These measurements are highly dependent on the radial location where the probe is placed, as suggested by Figs. 7(c) and 7(d), where radial profiles for the poloidal electric field and radial particle flux are depicted with and without biasing. The overall behavior of E_θ is similar to that exhibited by the floating potential, and the particle flux has a trend similar to the ion saturation current.

In a previous investigation on the effect of biasing on the MHD activity in TCABR (measured by Mirnov coils), two regimes with different effects of electrode bias were shown.²⁵ In one regime, the tokamak was configured to obtain a flat-top plasma current of $I_p \approx 100$ kA, such as that depicted in Fig. 2(a), without electrode biasing. In this regime the MHD activity does not grow naturally. By way of contrast, in the other regime (a typical profile being shown in Fig. 8) the ramp of plasma current is more slowly until it reaches a plateau (also at $I_p \sim 100$ kA), and high MHD activity is naturally obtained in this regime. As can be seen in Fig. 8, there is a high MHD activity starting at ~ 40 ms and remaining during ~ 20 ms. On inspecting Figs. 8(b) and 8(c), we also observe a slight increase in the plasma density due the growth of high MHD activity, as well as a clear change in the floating potential fluctuations.

In the course of the present investigation, discharges of both regimes were used to perform measurements of the floating potential, ion saturation current, poloidal electric field, and turbulence driven particle transport; and the corresponding data were subjected to RQA, the radial profile of DET being plotted in Figs. 9(a)–9(d), respectively. In both regimes, the measured signals are considered before and without high MHD activity. We observe that the radial profile of DET is virtually unchanged as discharges of both

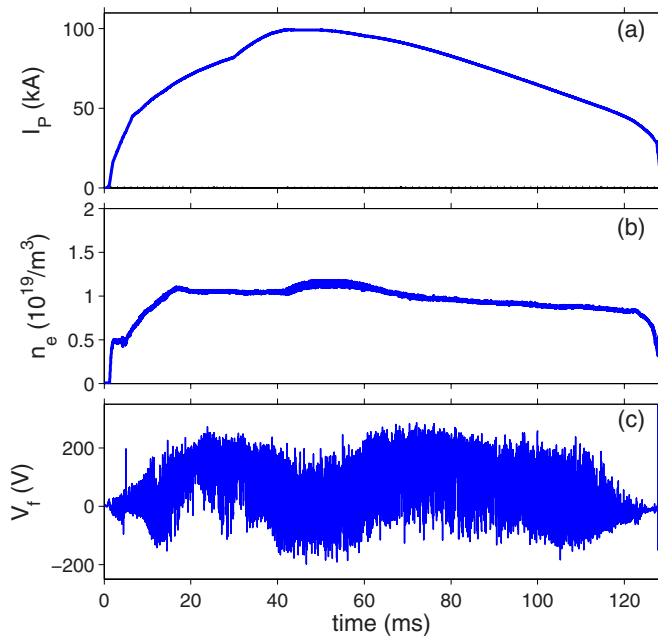


FIG. 8. (Color online) Time evolution of (a) plasma current, (b) electron density, and (c) floating potential for a typical discharge of TCABR tokamak in the second regime (no biasing).

regimes are considered. Moreover, these results indicate the good reproducibility of the RQA diagnostics, as well as the TCABR experimental conditions (once the two completely different sets of discharges were used and consistent profiles were observed for all the four considered data sets).

VI. CONCLUSIONS

RQA is a powerful approach for the investigation of nonlinear time series appearing in a variety of physically interesting applications, since RQA quantifies the number and duration of recurrences of a dynamical system presented by its phase space trajectory. One of the advantages from using RQA is to get measures for quantifying the information content even of turbulent signals. Those recurrence-based diagnostics, such as determinism, Shannon entropy, laminarity, trapping time, etc., reflect how predictable a system is.³⁸

The experimental time series considered in this paper are electrostatic potential fluctuations, ion saturation current, poloidal electric field and radial transport particle flux in the edge plasma of the TCABR tokamak, with and without electrode biasing. Although several quantitative diagnostics of recurrence were used, we found DET to be a sufficiently enlightening measure to quantify the variations in the dynamics of the analyzed plasma electrostatic fluctuations signals. In other words, the higher is DET for a measured time signal (within a given time window) the more predictable it is.

We found that, for the floating potential and poloidal electric field fluctuations, the values of DET decrease with the application of biasing at the edge region. For those signals, DET decreased the most where it was more pronounced within the plasma column, namely just before the plasma edge. As for the ion saturation current and turbulent flux data, DET also diminished with application of biasing, but

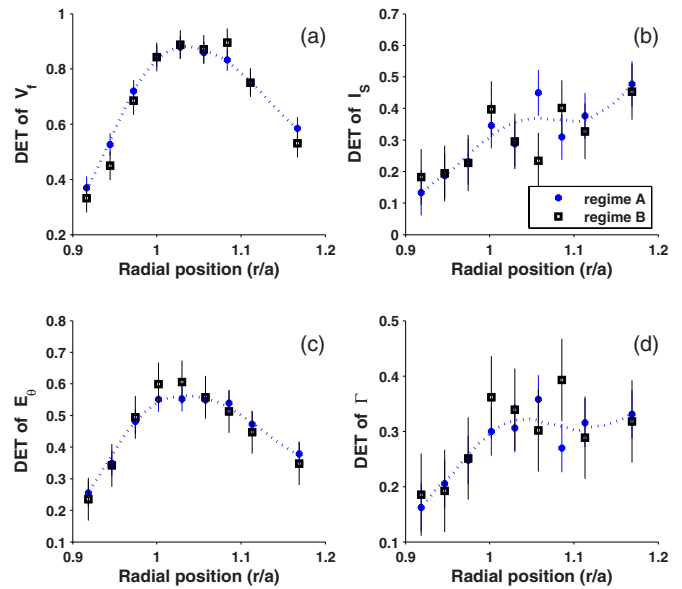


FIG. 9. (Color online) Radial profile of determinism for (a) floating potential, (b) fluctuating ion saturation current, (c) poloidal electric field, and (d) turbulence driven particle transport flux for regime A (circles) and regime B (squares) discharges of TCABR. In both regimes, signals are considered before biasing and with low magnetic activity.

this decrease did not occur with most intensity where it was most pronounced before biasing, since the maximum value of DET occurred at the scrape-off layer.

Another noteworthy feature of recurrence-based techniques is that it was capable of distinguish biased from non-biased discharges using windows as small as 1 ms. Moreover, the diagnostics we used (determinism, laminarity, entropy, etc.) gave consistent results in several plasma discharges, so as to give us confidence on the reproducibility of the results we reported in this work. In general, the values of the recurrent-based diagnostics presented a significant variation near the plasma edge and were proven to be remarkably sensitive to perturbations. In fact, the radial dependence of the electrostatic turbulence level at the vicinity of the plasma radius is a signature of the role played by radial density gradients in the generation of drift waves which is the essential cause of turbulence in the plasma edge. The presence of steep density gradients in the plasma edge can give rise to fully developed drift-wave turbulence.¹

The radial profiles for the poloidal electric field and the floating potential fluctuations were found to be very similar without biasing. The value of DET related to the poloidal electric field presents a significant reduction due to the biasing within a region more internal than for the floating potential. However the effect of biasing is quite different for those signals, despite one is obtained from the other. In addition, the ion saturation current and the radial particle flux have similar properties, with and without biasing. Hence the ion saturation current seems to be more important than the radial velocity fluctuations for the dynamics of the radial particle flux. Another interesting feature was that the reduction in DET did not occur at the same radial position of the biasing electrode but slightly after that point.

Two types of discharges were considered in our analysis.

In discharges of the first regime (or regime A, for short) the plasma current increases relatively fast and reaches a plateau approximately together with the electron density. For regime B discharges, however, the plasma current increases at a slower rate and reaches a plateau well after the electron density does. High MHD activity occurs spontaneously for regime B discharges, oppositely as for regime A discharges. The recurrence-based diagnostics we used in this work showed similar profiles for these two regimes in absence of high MHD activity. Hence the turbulence should exhibit a similar dynamics for both regimes A and B. As a consequence, the differences between both regimes may not be due to turbulence-related effects.

We proposed in this paper that the powerful tools provided by RQA should be useful, in general, to characterize plasma changes observed in experiments where some kind of plasma control is applied. This could be the case, for example, in discharges with ELM suppression,³⁹ turbulence modification by resonant divertors,⁴⁰ or even during abrupt changes occurring in the LH transition.⁴¹

ACKNOWLEDGMENTS

This work was made possible with partial financial help from FAPESP, CNPq, Fundação Araucária, CAPES, FINEP-RNP (Brazilian Fusion Network), and Contract No. SFB 555 (DFG), Université de Provence and PACA (Provence Alpes Côte d'Azur) Region. Z.O.G.-F. is the recipient of a bourse d'accueil de la Ville de Marseille.

¹W. Horton, *Rev. Mod. Phys.* **71**, 735 (1999).

²A. J. Wootton, B. A. Carreras, H. Matsumoto, K. McGuire, W. A. Peebles, Ch. P. Ritz, P. W. Terry, and S. J. Zweben, *Phys. Fluids B* **2**, 2879 (1990).

³C. Hidalgo, C. Alejalde, A. Alonso, J. Alonso, L. Almuquera, F. de Aragón, E. Ascasfbar, A. Baciero, R. Balbín, E. Blanco, J. Botija, B. Brañas, E. Calderón, A. Cappa, J. A. Carmona, R. Carrasco, F. Castejón, J. R. Cepero, A. A. Chmyga, J. Doncel, N. B. Dreval, S. Eguilior, L. Eliseev, T. Estrada, J. A. Ferreira, A. Fernández, J. M. Fontdecaba, C. Fuentes, A. García, I. García-Cortés, B. Gonçalves, J. Guasp, J. Herranz, A. Hidalgo, R. Jiménez, J. A. Jiménez, D. Jiménez-Rey, I. Kirpichev, S. M. Khrebtov, A. D. Komarov, A. S. Kozachok, L. Krupnik, F. Lapayese, M. Liniers, D. López-Bruna, A. López-Fraguas, J. López-Rázola, A. López-Sánchez, E. de la Luna, G. Marcon, R. Martín, K. J. McCarthy, F. Medina, M. Medrano, A. V. Melnikov, P. Méndez, B. van Milligen, I. S. Nedzelskiy, M. Ochando, O. Orozco, J. L. de Pablos, L. Pacios, I. Pastor, M. A. Pedrosa, A. de la Peña, A. Pereira, A. Petrov, S. Petrov, A. Portas, D. Rapisarda, L. Rodríguez-Rodrigo, E. Rodríguez-Solano, J. Romero, A. Salas, E. Sánchez, J. Sánchez, M. Sánchez, K. Sarkisian, C. Silva, S. Schepetov, N. Skvortsova, F. Tabarés, D. Tafalla, A. Tolkachev, V. Tribaldos, I. Vargas, J. Vega, G. Wolfers, and B. Zurro, *Nucl. Fusion* **45**, S266 (2005).

⁴A. J. Wootton, M. E. Austin, R. D. Bengtson, J. A. Boedo, R. V. Bravenec, D. L. Brower, J. Y. Chen, G. Cima, P. H. Diamond, R. D. Durst, P. H. Edmonds, S. P. Fan, M. S. Foster, J. C. Forster, R. Gandy, K. W. Gentle, R. L. Hickok, Y. X. Hey, S. K. Kim, Y. J. Kim, H. Lin, N. C. Luhmann, S. C. McCool, W. H. Miner, A. Ouroua, D. M. Patterson, W. A. Peebles, P. E. Phillips, B. Richards, C. P. Ritz, T. L. Rhodes, D. W. Ross, W. L. Rowan, P. M. Schoch, D. Sing, E. J. Synakowski, P. W. Terry, K. W. Wenzel, J. C. Wiley, X. Z. Yang, X. H. Yu, Z. Zhang, and S. B. Zheng, *Plasma Phys. Controlled Fusion* **30**, 1479 (1988).

⁵M. Baptista, I. L. Caldas, M. V. A. P. Heller, and A. A. Ferreira, *Phys. Plasmas* **10**, 1283 (2003).

⁶P. J. Morrison and B. A. Shadwick, *Commun. Nonlinear Sci. Numer. Simul.* **13**, 130 (2008).

⁷B. N. Kuvshinov and T. J. Schep, *Phys. Rev. Lett.* **84**, 650 (2000).

⁸Y. Xu, R. R. Weynants, S. Jachmich, M. Van Schoor, M. Vergote, P.

Peleman, M. W. Jakubowski, M. Mitri, D. Reiser, B. Unterberg, and K. H. Finken, *Phys. Rev. Lett.* **97**, 165003 (2006).

⁹N. Marwan and J. Kurths, *Phys. Lett. A* **302**, 299 (2002).

¹⁰Z. O. Guimarães-Filho, I. L. Caldas, R. L. Viana, J. Kurths, I. C. Nascimento, and Yu. K. Kuznetsov, *Phys. Lett. A* **372**, 1088 (2008).

¹¹J. P. Eckmann, S. O. Kamphorst, and D. Ruelle, *Europhys. Lett.* **4**, 973 (1987).

¹²M. Casdagli, *Physica D* **108**, 12 (1997).

¹³C. L. Webber and J. P. Zbilut, *J. Appl. Physiol.* **76**, 965 (1994).

¹⁴N. Marwan, M. H. Trauth, M. Vuille, and J. Kurths, *Clim. Dyn.* **21**, 317 (2003).

¹⁵J. A. Holyst, M. Zebrowska, and K. Urbanowicz, *Eur. Phys. J. B* **20**, 513 (2001).

¹⁶J. Kurths, U. Schwarz, C. P. Sonett, and U. Parlitz, *Nonlinear Processes Geophys.* **1**, 72 (1994); N. Marwan, M. Thiel, and N. R. Nowaczyk, *ibid.* **9**, 325 (2002).

¹⁷N. Marwan, N. Wessel, U. Meyerfeldt, A. Schirdewan, and J. Kurths, *Phys. Rev. E* **66**, 026702 (2002).

¹⁸T. K. March, S. C. Chapman, and R. O. Dendy, *Geophys. Res. Lett.* **32**, L04101, doi:10.1029/2004GL021677 (2005); *Physica D* **200**, 171 (2005).

¹⁹R. O. Dendy and S. C. Chapman, *Plasma Phys. Controlled Fusion* **48**, B313 (2006).

²⁰R. M. O. Galvão, V. Bellintani, Jr., R. D. Bengtson, A. G. Elfmov, J. I. Elizondo, A. N. Fagundes, A. A. Ferreira, A. M. M. Fonseca, Yu. K. Kuznetsov, E. A. Lerche, I. C. Nascimento, L. F. Ruchko, W. P. de Sá, E. A. Saettoni, E. K. Sanada, J. H. F. Severo, R. P. da Silva, V. S. Tsypin, O. C. Usuriaga, and A. Vannucci, *Plasma Phys. Controlled Fusion* **43**, A299 (2001).

²¹A. A. Ferreira, M. V. A. P. Heller, I. L. Caldas, E. A. Lerche, L. F. Ruchko, and L. A. Baccalá, *Plasma Phys. Controlled Fusion* **46**, 669 (2004).

²²W. Horton and A. Hasegawa, *Chaos* **4**, 227 (1994).

²³G. Z. dos Santos Lima, Z. O. Guimarães-Filho, I. L. Caldas, I. C. Nascimento, Yu. K. Kuznetsov, A. M. Batista, S. R. Lopes, and R. L. Viana, *Phys. Plasmas* **16**, 042508 (2009).

²⁴I. C. Nascimento, Yu. K. Kuznetsov, J. H. F. Severo, A. M. M. Fonseca, A. Elfmov, V. Bellintani, M. Machida, M. V. A. P. Heller, R. M. O. Galvão, E. K. Sanada, and J. I. Elizondo, *Nucl. Fusion* **45**, 796 (2005).

²⁵I. C. Nascimento, Yu. K. Kuznetsov, Z. O. Guimarães-Filho, I. El Chamaa-Neto, O. Usuriaga, A. M. M. Fonseca, R. M. O. Galvo, I. L. Caldas, J. H. F. Severo, I. B. Semenov, C. Ribeiro, M. V. A. P. Heller, V. Bellintani, J. I. Elizondo, and E. Sanada, *Nucl. Fusion* **47**, 1570 (2007).

²⁶F. Takens, in *Dynamical Systems and Turbulence, Warwick 1980*, Vol. 898, edited by D. A. Rand and L. S. Young (Springer-Verlag, Berlin, 1981).

²⁷H. Kantz and T. Schreiber, *Nonlinear Time Series Analysis* (Cambridge University Press, Cambridge, 1997).

²⁸F. M. Atay and Y. Altintas, *Phys. Rev. E* **59**, 6593 (1999).

²⁹M. Thiel, M. C. Romano, and J. Kurths, *Phys. Lett. A* **330**, 343 (2004).

³⁰J. P. Zbilut and C. L. Webber, Jr., *Phys. Lett. A* **171**, 199 (1992).

³¹N. Marwan, M. C. Romano, M. Thiel, and J. Kurths, *Phys. Rep.* **438**, 237 (2007).

³²Freely available software for obtaining RPs and performing RQA is listed in <http://www.recurrence-plot.tk/programmes.php>.

³³L. L. Trulla, A. Giuliani, J. P. Zbilut, and C. L. Webber, Jr., *Phys. Lett. A* **223**, 255 (1996).

³⁴E. Ott, *Chaos in Dynamical Systems* (Cambridge University Press, Cambridge, 1992).

³⁵S. J. Camargo, B. D. Scott, and D. Biskamp, *Phys. Plasmas* **3**, 3912 (1996).

³⁶A. Hasegawa and M. Wakatani, *Phys. Rev. Lett.* **50**, 682 (1983).

³⁷C. Rodrigues Neto, Z. O. Guimaraes-Filho, I. L. Caldas, I. C. Nascimento, and Yu. K. Kuznetsov, *Phys. Plasmas* **15**, 082311 (2008).

³⁸S. Schinkel, N. Marwan, O. Dimyer, and J. Kurths, *Phys. Lett. A* **373**, 2245 (2009).

³⁹M. J. Schaffer, J. E. Menard, M. P. Aldan, J. M. Bialek, T. E. Evans, and R. A. Moyer, *Nucl. Fusion* **48**, 024004 (2008).

⁴⁰K. H. Finken, T. E. Evans, D. Reiter, K. H. Spatschek, and W. Suttrop, *Nucl. Fusion* **48**, 024001 (2008).

⁴¹S. E. Sharapov, F. M. Poli, and JET-EFDA Contributors, in *35th EPS Conference on Plasma Physics*, Europhysics Conference Abstracts Vol. 32D, Hersonissos, 2008, edited by P. Lalouis and S. Moustazis (European Physical Society, Lausanne, 2008), p. 4.071.